Hyperelastic-plastic materials,
Large deformation theory, FEM

GAJEWSKI Marcin[1]

APPLICATION OF THE THEORY OF HYPERELASTIC-PLASTIC MATERIALS IN THE TEST OF STATIC STRETCHING OF THE ROD WITH CIRCULAR CROSSECTION

The issue of necking in the stretched elements is widely debated in the literature. In these works the results of experimental studies, analytical solutions and the FEM simulations in the framework of the theory of large deformation theory can be found, cf. e.g.[6]. Here the effective solutions of boundary value problems are obtained with application of finite element method (FEM) and ABQAQUS software. It is worth noting that reasonable modeling of rod stretching experiment in frame of the small deformation theory is not possible. The main goal of this study is to compare the FEM solutions obtained for two different large deformation theories for elastic-plastic materials, i.e. the theoretical formulation proposed in [5] and the theory implemented in ABAQUS/Standard[1].

ZASTOSOWANIE TEORII HIPERSPRĘŻYSTO-PLASTYCZNOŚCI W STATYCZNEJ PRÓBIE ROZCIĄGANIA PRĘTA O PRZEKROJU KOŁOWYM

Zagadnienie powstawania przewężenia zwanego szyjką w elementach rozciąganych jest szeroko dyskutowane w literaturze dotyczącej teorii plastyczności. W pracach tych zamieszczono wyniki badań doświadczalnych, rozwiązania analityczne oraz symulacje MES, por. np.[6]. W tej pracy do rozwiązania zagadnienia brzegowego efektywnie stosuje się metodę elementów skończonych (MES) i program ABAQUS. Warto podkreślić już na wstępie, że racjonalne modelowanie tego eksperymentu w ramach teorii sprężysto-plastyczności małych deformacji nie jest możliwe. Celem tej pracy jest porównanie rozwiązań MES zadania rozciągania pręta przy zastosowaniu dwóch różnych teorii sprężysto-plastyczności dla dużych deformacji, tzn. sformułowania teoretycznego zaproponowanego w [5] oraz teorii zaprogramowanej w systemie ABAQUS/Standard[1].

1. INTRODUCTION

The issue of necking in the stretched elements is widely debated in the literature, see eg [4], [5]. In these works the results of experimental studies, analytical solutions and the FEM simulations in the framework of the theory of large deformation theory can be found. Also in the monograph of Simo and Hughes [6] the results of experimental and numerical tests

[1] Marcin Gajewski, Politechnika Warszawska, Wydział Inżynierii Lądowej, Zakład Wytrzymałości Materiałów, Teorii Sprężystości i Plastyczności, Armii Ludowej 16, 00-637 Warszawa, Polska, Tel. (+4822) 2345754, E-mail: m.gajewski@il.pw.edu.pl

with application of the theory of elastic-plastic large deformation materials are presented. These tests are carried out taking into account the influence of the strain rate or as the static test. For effective solution of the boundary value problem or initial boundary value problem the finite element method (FEM) is applied. It is worth noting that the rational modeling of this experiment in the theory of small elastic-plastic deformation is not possible.

The purpose of this study is to compare the solutions of the task of rod stretching using two different formulations of theory for large deformation for elastic-plastic materials, i.e. the results obtained for large deformation theory with hyperelastic-plastic model (cf. [5]) and the theory for relatively large deformation available in ABAQUS / Standard [1]. The hyperelastic-plastic constitutive model of metals presented below is incorporated in ABAQUS/ Standard, by UMAT Subroutine written in FORTRAN language.

Numerical solutions of static task of rod stretching are carried out for different FEM discretizations of the body. In the static task the assumption of axial symmetry and the symmetry with respect to the plane perpendicular to the axis of the bar and dividing it into two equal parts are incorporated. However, such assumptions may cause *a priori*, that we are not able to find some solutions that are possible within the theory of large deformation, see the comments in the monograph [2]. Assumption of deformation symmetry in the static task are allowed and can be interpreted as the lack of imperfection shape and material inhomogeneities.

2. CONSTITUTIVE MODEL OF HYPERELASTIC-PLASTIC MATERIAL

Constitutive model was formulated in frame of large deformation theory with consequent multiplicative decomposition of gradient of deformation tensor into two parts: an elastic and plastic one denoted respectively as $\mathbf{F}_e$ and $\mathbf{F}_p$. Additionally each of deformation tensors was decomposed with application of polar decomposition theorem onto part describing stretching (right and left stretch tensor denoted respectively as $\mathbf{U}$ and $\mathbf{V}$) and part connected with the rotation of the material point ($\mathbf{R}$). It was assumed that plastic deformation has no volumetric change, what is a reasonable assumption in case of metallic materials and gives $\det\mathbf{F}_p = \det\mathbf{C}_p = ... = \det\mathbf{V}_p = 1$. The elastic properties of materials are described with application of hyperelastic model of the MCMH type, cf. [2,3]. In this model the stored energy function, which is a potential for the stress tensor can be written in the following form:

$$W = \frac{\mu_0}{2}\left(\bar{I}_{e1} - 3\right) + \hat{\alpha}\left(J_e\right) \ , \tag{1}$$

where: μ_0 - shear modulus in reference configuration,

$\bar{I}_{e1}$ - an invariant equal to $\bar{I}_{e1} = J_e^{-\frac{2}{3}}\mathrm{tr}\mathbf{U}^2$,

J_e - an invariant equal to $J_e = \det\mathbf{F}_e$,

$\hat{\alpha}\left(J_e\right)$ - describes the volumetric changes.

The function $\hat{\alpha}\left(J_e\right)$ can be expressed in the following manner:

$$\hat{\alpha}(J_e) = \frac{K_0}{4}\left[(J_e - 1)^2 + (\ln J_e)^2\right]. \tag{2}$$

where: K_0 - volumetric stiffness modulus in reference configuration.

The plastic properties are taken into account by postulating associative plasticity with yield condition analogical to the well-known Huber-Mises condition with isotropic hardening:

$$f(\boldsymbol{\tau}, \alpha) = \|\boldsymbol{\tau}_d\| - \sqrt{\frac{2}{3}} k(\alpha) = 0, \tag{3}$$

where: $\boldsymbol{\tau}$ - Kirchhoff stress tensor,
$\|\boldsymbol{\tau}_d\|$ - the norm of deviatoric part of Kirchhoff stress tensor,
$k(\alpha)$ - hardening function.

The hardening function in (3) can be expressed in the following manner:

$$k(\alpha) = \sigma_Y + A\alpha + (A_\infty - A_0)\left(1 - e^{-\alpha\delta}\right). \tag{4}$$

where: σ_Y - yield stress in the uniaxial test,
A, A_0, A_∞, δ - hardening parameters.

In (3) $\boldsymbol{\tau}_d$ is a deviatoric part of the Kirchhoff stress tensor, and function $k(\alpha)$, describes an isotropic nonlinear strain hardening behavior calibrated from simple stretching test. In the variable α the history of the plastic deformation (via $\overline{\dot{\mathbf{C}}}_p$) can be taken into account.

3. A COMPARISON OF FEM SIMULATION RESULTS FOR TWO DIFFERENT FORMULATIONS OF PLASTICITY WITH EXPERIMENTAL DATA

As it was mentioned in the introduction, the static rod stretching test was analyzed in [5] and in the monograph [6]. Here the same geometrical and material data are taken into account, in order to compare obtained results. So, it was assumed that the rod with circular cross-section and radius $r = 6.413\,[\text{mm}]$ is $l = 53.334\,[\text{mm}]$ long.

The initial elastic properties are characterized by shear modulus μ_0 =80.1938 [GPa] and volumetric stiffness modulus K_0 =164.206 [GPa], what rewritten into Young modulus and Poisson ratio gives $E = 206.9$ [GPa] and $\nu = 0.29$. In (4) the following data are describing the strain hardening process: A =0.12924 [GPa], A_∞ =0.715 [GPa], A_0 =0.45 [GPa], σ_Y =0.45 [GPa] and δ =16.93, cf. fig. 1.

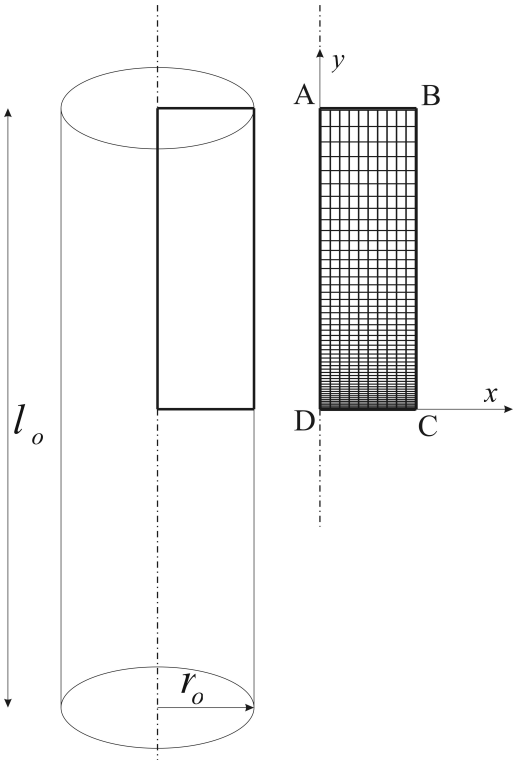

Fig.1.Geometry of the rod, symmetry assumptions and FEM model

The stretching of the rod was carried out with application of displacement boundary conditions. At the edge DC the displacement in y direction is blocked, while at the edge AB the displacement in the x direction is blocked and displacement in y direction is set to 7[mm]. At the edge AD the boundary conditions result from axial symmetry, and for BC edge the zero stress boundary conditions are assumed.

The task was solved for constitutive model presented in paragraph 2 and incorporated into the ABAQUS/ Standard, via UMAT Subroutine written in FORTRAN language.

The same task was solved with application of plasticity with additive decomposition of logarithmic strain tensor. In that formulation the yield condition is written in terms of deviatoric part of Cauchy stress tensor, and the nonlinear isotropic hardening was modeled by piecewise-linear function. So from theoretical point of view that constitutive model is substantially different from the hyperelastic-plastic model. Nonetheless the results of the analysis should be consistent, because of the fact that elastic deformations and local material particle rotation in analyzed task were relatively small. Furthermore the differences between components of the Cauchy and Kirchhoff stress tensors shouldn't be significantly different because under assumption about incompressibility of the plastic part of deformation the relationship hold $\boldsymbol{\tau} = J_e \boldsymbol{\sigma}$. Additionally we know that initial shear modulus is about two orders of magnitude higher than shear yield, what is typical for metals.

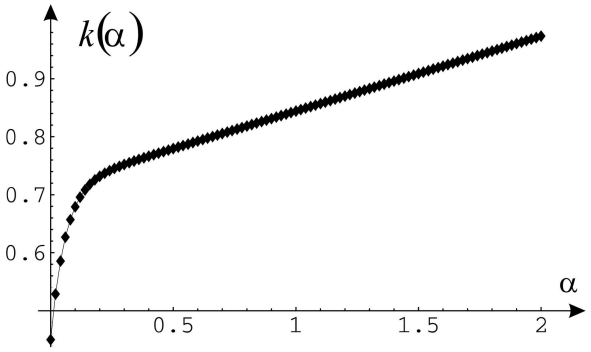

Fig.2. Approximation of function $k(\alpha) \equiv \sigma_p(\varepsilon_p)$ *with linear segments*

The properties of isotropic and nonlinear plastic hardening were assumed according to the graph presented in fig.2 as an linear approximation in a hundred equal intervals. It means that there is the following relationship $k(\alpha) \equiv \sigma_p(\varepsilon_p)$, where $\varepsilon_p = \int_0^t \sqrt{\frac{2}{3}} \left\| \dot{\bar{\mathbf{e}}}_p(\bar{\eta}) \right\| \mathrm{d}\bar{\eta}$ (equivalent plastic strain).

The FEM mesh is the same for both tasks and consists of 10x50=500 CAX4 type elements with linear shape functions. The mesh has higher density near the symmetry line, cf. fig.1. The task was solved with use of automatic step division procedure and 130 iterations were needed to obtain solution with assumed accuracy.

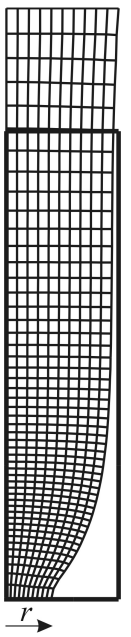

Fig.3. Deformed mesh 10x50 elements

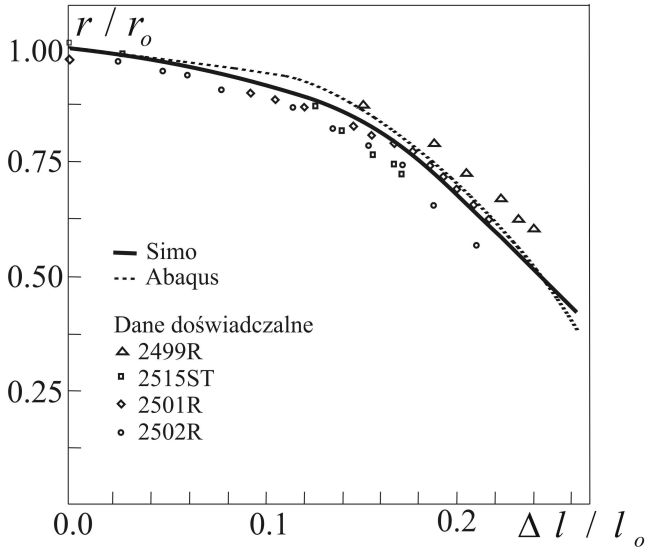

Ratio of current radius in DC section and initial radius as a function of $\Delta l / l_o$ *- results comparison, cf. also[6]*

The results of the rod deformation are presented in fig.3. In turn in fig. 4 the comparison of FEM results for both formulations and experimental data are shown. In fig.3, 6 and 7 the

results are presented at the end of active process (without an elastic unloading process). In fig.5 the contour graph of equivalent Mises stresses is presented at the end of loading step (a) and after unloading (b). Differences between the results obtained by two different formulations of elasto-plasticity are, from the standpoint of conformity with experimental data irrelevant. Just as in the work [5] we have checked the influence of the number of mesh elements on the results showing that it is negligible. The same tasks were solved with the denser mesh of 20x100= 2000 elements. Obtained results are practically identical with an accuracy of at least two significant digits.

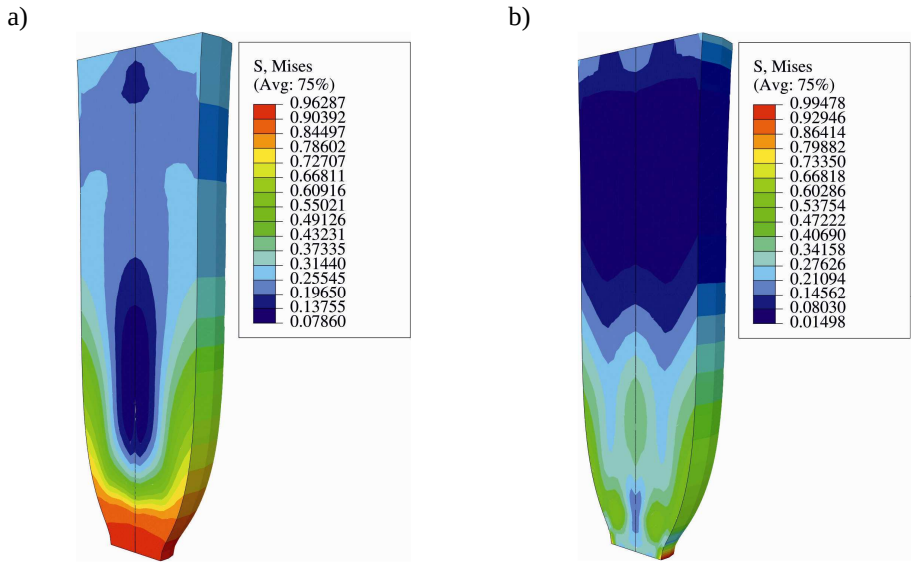

Fig.5. Example of FEM results (ABAQUS)- contour graphs: a) equivalent Mises stress at the end of loading step, b) equivalent Mises stress after unloading

Exemplary results are presented as contour plots in Figure 5-7. Significant deformations and concentration of plastic strain occurs naturally in the neck, see fig.3 and 6. The fields of displacement norm, stress and strain components are highly heterogeneous on the length of the sample as well as on its diameter. The highest effective stresses are located in the neck of the sample and are about 0.96 [GPa] and decrease uniformly in the direction of the upper edge, see fig.5. The equivalent plastic strain outside the neck are about four orders of magnitude smaller, than in the neck, cf. fig.6a. The largest plastic deformation occur in the neck and along the axis of the rod, and in the total strain, crucial contribution have the plastic strain. It may be noted that extreme elastic strain are of at least three orders of magnitude smaller than plastic strains. The distribution of elastic strain on the height and radius of the sample is more heterogeneous than that for plastic strain. It is easy to check that in the plastic range the assumption of incompressibility is met with a high accuracy.

a) b)

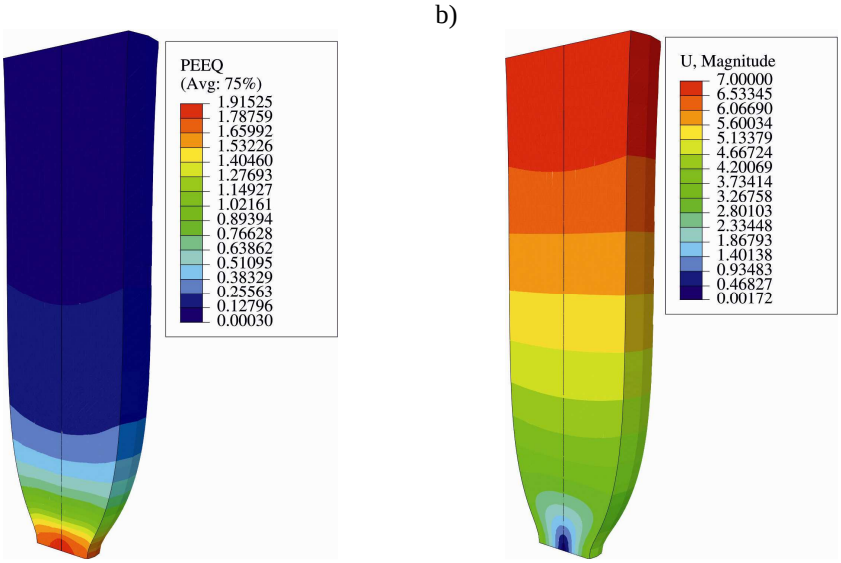

Fig.6. Example of FEM results (ABAQUS)- contour graphs: a) equivalent plastic strain, b) norm of displacement at the end of loading step

a) b)

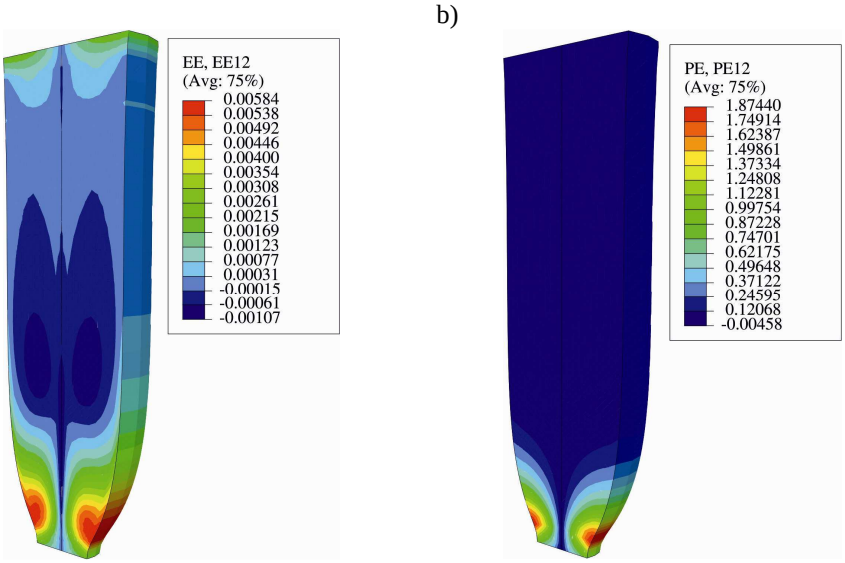

Fig.7. Example of FEM results (ABAQUS)- contour graphs: a) shearing component of elastic strain, b) shearing component of plastic strain at the end of loading step

4. CONCLUSIONS

The formulation presented in the work [5] and implemented by author should be regarded as consistent, cf. [3], while the standard formulation implemented in ABAQUS and based on an additive decomposition of logarithmic strain measure can not be used for significantly large deformation of the body. The manual [1] state limitation onto the elastic part of strain (up to about 5%). Plastic deformation and rotation of particles of the body are not at all limited. Based on the elaboration presented in [3], it can be concluded that in the case of deformation in which there are significant local rotations of particles of the body, part of the deformation gradient describing the rotation should be limited. Another very important issue in this implementation is the answer to the question whether the elastic behavior of the material model is close to linear. If we are dealing with non-linear elasticity that the results will certainly be irrational. Summary calculation example shows, however, that in many applications where local rotations are small and the behavior of the material to yield is almost linear ABAQUS program with its standard formulation can be reasonably used.

5. REFERENCES

[1] ABAQUS *Theory manual*, Version 6.1., Hibbitt, Karlsson and Sorensen, Inc., Pawtucket, 2000.
[2] Jemioło S., *Studium hipersprężystych własności materiałów izotropowych. Modelowanie i implementacja numeryczna*, Prace Naukowe, Budownictwo z. 140, str. 1-308, Warszawa 2002.
[3] Jemioło S., Gajewski M., Duże deformacje sprężysto-plastyczne w anizotropowych metalach, Raport z grantu dziekańskiego WIL PW, Warszawa 2004
[4] Malinin M.N., Rżysko J.: *Mechanika materiałów*, PWN, Warszawa, 1981.
[5] Simo J.C., A framework for finite strain elastoplasticity based on maximum plastic dissipation and the multiplicative decomposition. Part II: Computational aspects, Comp. Methods Appl. Mech. Engin., vol. 68, pp. 1-31, 1988.
[6] Simo J.C., Hughes T. J. R., *Computational inelasticity*, Springer- Verlag, Inc., New York, 1998.
[7] Simo J.C., Pister K.S.: Remarks on rate constitutive equations for finite deformation problems: Computational implications, Computer Methods in Applied Mechanics and Engineering, 46, pp. 201-215, 1984.
[8] Simo J.C., Taylor R.L.: Consistent tangent operators for rate independent elasto-plasticity, Computer Methods in Applied Mechanics and Engineering, 48, pp. 101-118, 1985.